http://doi.org/10.18321/ectj663

Development of a Technique and Investigation of Capacitance Characteristics of Electrode Materials for Supercapacitors Based on Nitrogen-Doped Carbon Nanotubes

G.Yu. Simenyuk[1*], A.V. Puzynin[1,2], O.Yu. Podyacheva[3], A.V. Salnikov[1,3], Yu.A. Zakharov[1,4], Z.R. Ismagilov[1,3]

[1]Institute of Coal Chemistry and Materials Science SB RAS, Pr. Sovetskiy, 18, Kemerovo, 650000, Russia
[2]T.F. Gorbachev Kuzbass State Technical University, 50 Let Oktyabrya str., 17, Kemerovo, 650000, Russia
[3]Boreskov Institute of Catalysis SB RAS, Pr. Akad. Lavrentieva, 5, Novosibirsk, 630090, Russia
[4]Kemerovo State University, Krasnaya str., 6, Kemerovo, 650043, Russia

Article info

Received:
8 January 2017

Received in revised form:
26 March 2017

Accepted:
18 May 2017

Keywords:
Electrode materials
Supercapacitors
Electric capacitance
Electrical double layer
Pseudocapacitance
Carbon nanotubes

Abstract

Carbon nanotubes are widely employed as catalyst supports and electrode materials. In our earlier studies, capacitance characteristics of carbon nanotubes (CNTs) and nitrogen-doped carbon nanotubes (N-CNTs) were measured. Voltammetric curves obtained for nitrogen-doped nanotubes in an acid electrolyte showed pseudocapacitance peaks that were caused by electrochemical processes involving nitrogen-containing functional groups. In this study, measurements were made in a two-electrode cell of a supercapacitor with a hydrophilic polypropylene PORP-A1 film serving as a separator in alkaline (6 M KOH solution) and acid (1 M H_2SO_4 solution) electrolytes using a PARSTAT 4000 potentiostat/galvanostat. A technique was developed to estimate the contribution of electrical double layer (EDL) by subtracting pseudocapacitance from total capacitance of a cell using the Origin 9 software. The contribution of EDL and pseudocapacitance to the capacitance of supercapacitor cells was estimated. The highest capacitance of an electrode material equal to 97.2 F/g (including the EDL capacitance of 65 F/g) was reached for nanotubes doped with 8.5% of nitrogen in an acid electrolyte at a potential scanning rate of 10 mV/s.

1. Introduction

Carbon nanotubes (CNTs) are promising materials for a wide application in flexible electronics, nanoelectronics and devices for energy conversion and storage. This is related to unique physicochemical properties of CNTs: high mobility of charge carriers, high thermal and electric conductivity, high specific surface area, mechanical strength and flexibility combined with chemical stability [1–8]. Nitrogen doping affects the mechanical, optical, electrical and adsorption properties of nanotubes, thus substantially extending the field of their application [7–13].

One of the most topical and promising application fields of carbon nanotubes is the development of electrode materials for supercapacitors (SC). When nanotubes are used as an electrode material, charge accumulation occurs due to formation of electrical double layer at the electrode/electrolyte interface and due to pseudocapacitance. Pseudocapacitance may be caused by the presence of oxygen- or nitrogen-containing groups and admixtures of catalysts – compounds of transition metals (Fe, Co, Ni, Cu, etc.) on the surface of nanotubes accessible to electrolyte ions.

In the case of nitrogen doping of nanotubes, it is very important to estimate the contribution of nitrogen to EDL capacitance and pseudocapacitance.

A technique has been developed for estimating the contribution of EDL to the total capacitance by subtraction of pseudocapacitance from total capacitance on voltammetric curves using the Origin software. The measurements were carried out in a two-electrode SC cell by cyclic voltammetry in a potential window from –1 to +1 V at a potential scanning rate of 10, 20, 40 and 80 mV/s in different electrolytes.

*Corresponding author. E-mail: galina-simenyuk@yandex.ru

Undoped (CNTs) and nitrogen-doped (N-CNTs) carbon nanotubes with the nitrogen content 2.0, 3.6, 6.0 and 8.5 wt.%, which were synthesized in our previous studies [14–16], served as the electrode materials. The effect of nitrogen doping of the nanotubes on electrical double layer capacitance, pseudocapacitance and total capacitance of electrode materials was studied.

2. Experimental

A special SC cell was designed for the experiments. Its construction is displayed on Fig. 1.

The cell casing consists of two cylinders (1) ground out of fluoroplastic, which are separated by a separator (2) and contracted by four pins (3) that are covered with insulating adhesive (4). Contracting plates (springs) (5) are located at an angle of 90° to each other. An electrode material sample mixed with an electrolyte is placed in holes (6) with the diameter of 6 mm and slowly compressed by special graphite cylinders (7) using plates (5). Wires (8), which apply a voltage to the electrodes, are connected to two pins.

SC electrode materials were synthesized by the following procedure: the tested carbon nanotubes were held at a residual pressure of inert gas (argon) 0.1 atm for an hour at 105 °C, then placed in an exiccator with $CaCl_2$ and cooled to room temperature for 2 h in an argon atmosphere. The tested 10 mg sample was supplemented with 3–4 drops of an aqueous 1 M solution of H_2SO_4 or 6 M solution of KOH, carefully ground in an agate mortar to a homogeneous paste-like state, and the resulting suspension was placed in SC holes as indicated above. A hydrophilic polypropylene PORP-A1 film was used as a separator.

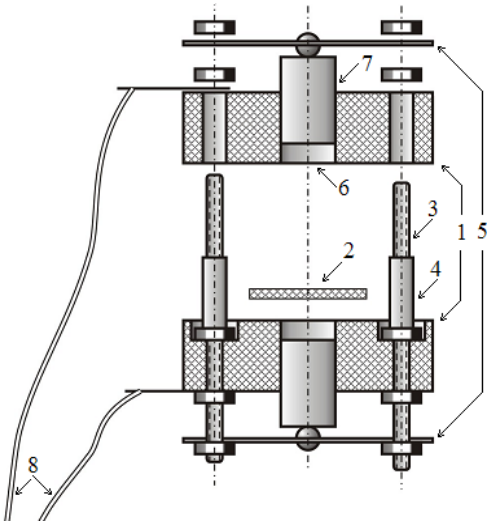

Fig. 1. Experimental SC cell for capacitance measurements: 1 – fluoroplastic cylinders; 2 – separator; 3 – stud pins; 4 – insulating adhesive; 5 – contracting plates (springs); 6 – holes for electrodes; 7 – graphite cylinders; 8 – wires.

The SC cell was connected to a PARSTAT 4000 measuring-feeding device, the data array from which was automatically transferred to a computer via a USB port and processed using the VersaStudio software.

Electrode characteristics were measured by cyclic voltammetry (CVs) in a potential window from –1 to +1 V at different potential scanning rates: 10, 20, 40 and 80 mV/s. The samples were examined using a symmetric design of the cell in which both the main electrode and the counter electrode were made of the same material. The measurements were used to obtain the voltammetric dependences, from which an electrode cell capacitance was calculated by formula (1). Capacitance of the electrode material in the symmetric cell was calculated by formula (2).

$$C_{cell} = \int I(U)dU/mv\Delta V \quad (1)$$

$$C_{el} = 2\ C_{cell} \quad (2)$$

where C_{cell} is the capacitance of the electrode cell; C_{el} is the capacitance of the tested electrode material; m is the mass of an electrode material; v is the scanning rate (V/s); ΔU is the potential window, V; and $\int I(U)dU$ is the area limited by the CVs curve.

For supercapacitors with energy accumulation in the electrical double layer, the typical shape of CVs curves is nearly rectangular. Such a shape is observed for the initial nanotubes in both the acid and alkaline electrolytes. In the case of nitrogen-doped nanotubes in the alkaline electrolyte (6 M KOH), distinct pseudocapacitance peaks are also not observed and shape of the curves is close to rectangular. In the acid electrolyte, distinct pseudocapacitance peaks appear on CVs curves of nitrogen-doped nanotubes; the area of the peaks increases with the nitrogen content. Hence, they are caused mostly by electrochemical redox processes involving nitrogen-containing functional groups on the surface of carbon nanotubes. It was assumed that the rectangular region is the contribution from EDL, and peaks in the horizontal regions of CVs curves are caused by pseudocapacitance: $C_{total} = C_{EDL} + C_{PC}$, where C_{total} is the total capacitance, C_{EDL} is the capacitance of electrical double layer, and C_{PC} is the pseudocapacitance. To estimate the

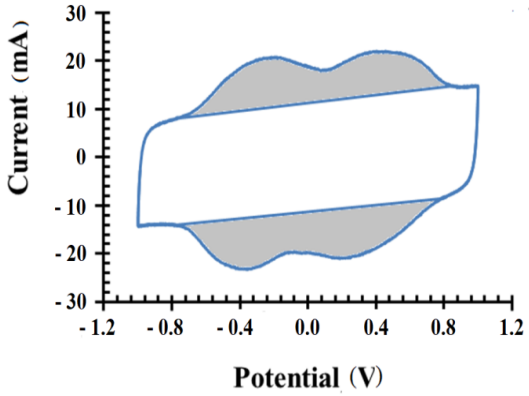

Fig. 2. CVs curves for the cells (exemplified by N-CNTs-8.5) in the acid electrolyte at a potential scanning rate of 80 mV/s. The contribution of pseudocapacitance is colored gray.

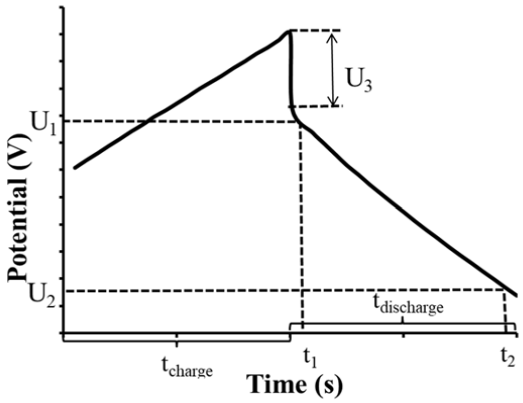

Fig. 3. The first cycle of galvanostatic charge-discharge curve of a supercapacitor cell.

contribution from EDL, the area of pseudocapacitance peaks was subtracted from the total area limited by CVs curves using the Origin 9 program, i.e. the area of the 'rectangular' region without peaks was determined by extrapolation of the horizontal regions, and the EDL capacitance was calculated.

Figure 2 displays a typical voltammetric dependence for SC with the electrodes based on nitrogen-doped nanotubes (exemplified by N-CNTs-8.5) at a potential scanning rate of 80 mV/s; gray color indicates the region of pseudocapacitance peaks that is subtracted to estimate the contribution of EDL from the total area limited by CVs curves.

Galvanostatic charge-discharge (GSCD) curves were plotted using the chronopotentiometry method [17–20] – changes of the cell potential with time were recorded at the constant strength of current of charging (I_{charge} = + 10 mA) and discharging ($I_{discharge}$ = – 10 mA) processes and charge/discharge time (t_{charge} = $t_{discharge}$ = 10 s). Graphical representation of the charge-discharge curves is displayed on Fig. 3.

At the beginning of discharge curves, a sharp U_3 region is observed, which is caused by internal resistance of the cell (capacitance losses for internal resistance).

Equivalent series resistance (R) and capacitance of the cell (C) were found from galvanostatic charge curves by the formulas [19]:

$$R = U_3/I_{discharge}$$

$$C = -I_{discharge} \cdot (t_2 - t_1)/(U_2 - U_1) \cdot m$$

where U_1 and U_2 are the potential values at the discharge time t_1 and t_2, respectively, and m is the mass of an electrode material, g.

Internal resistance values can differ from specific electric resistance of a material because conductivity takes into account only the active component of electrode material, whereas internal resistance takes into account the active component of electrode material, electrolyte solution, separator, current collectors, diffusion limitations on charge transfer at the electrode/electrolyte interface, etc.

Measurements of electrochemical cells by impedometry were performed with sinusoidal alternating current [21–22] in the frequency range from 10^{-2} to 10^4 Hz. Electrical impedance of a supercapacitor comprises the active (real) component Z_{re} (electric resistance of electrode materials, separator, electrolyte and current collectors), which is virtually independent of frequency, and the reactive (imaginary) component Z_{im} (capacitive reactance), which depends on the current frequency.

Redox processes on the electrode surfaces are related to diffusion delivery/removal of ions from the solution volume and back. In this case, the so-called Warburg impedance [21] additionally emerges. Such impedance is denoted by a special symbol W and implies a series connection of resistance and capacitance, which depend on frequency ω (Fig. 4).

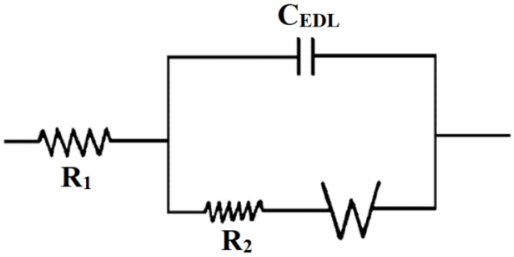

Fig. 4. An equivalent scheme for an electrode with capacitance of the double layer CEDL and uncompensated resistance of solution R_1. Resistance of the reaction consists of the charge transfer resistance R_2 and the Warburg impedance W.

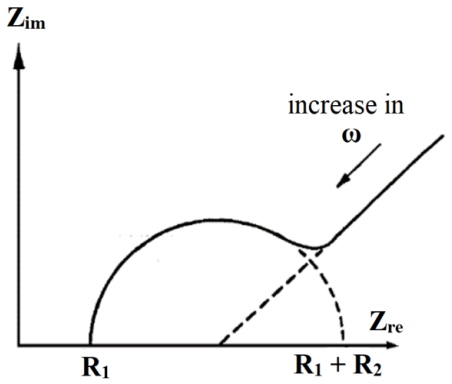

Fig. 5. The dependence of the reactive component of impedance on the active component for the equivalent scheme displayed on Fig. 4.

In this case (Fig. 5), the semicircle has the center $Z_{re} = R_1 + R_2/2$ with the radius $R_2/2$. Overall, the diagram demonstrates the presence of both the kinetic control (semicircle) and the diffusion-controlled region (a straight line with a single slope). The shape of the diagram can change in dependence on the tested system and measurement mode [21].

3. Results and Discussion

3.1. Investigation of electrode materials by cyclic voltammetry

Carbon electrodes of symmetric SC cells accumulate charge mostly due to EDL. The contribution from pseudocapacitance of oxygen- and nitrogen-containing surface functional groups to the total capacitance is caused by their type (carboxyl, phenol, lactone, hydroxyl, amine and other groups), percentage, electrochemical activity and accessibility to electrolyte solutions.

Experimental CVs curves for symmetric cells with undoped (CNTs) and nitrogen-doped (exemplified by N-CNTs-8.5) carbon nanotubes are displayed on Fig. 6.

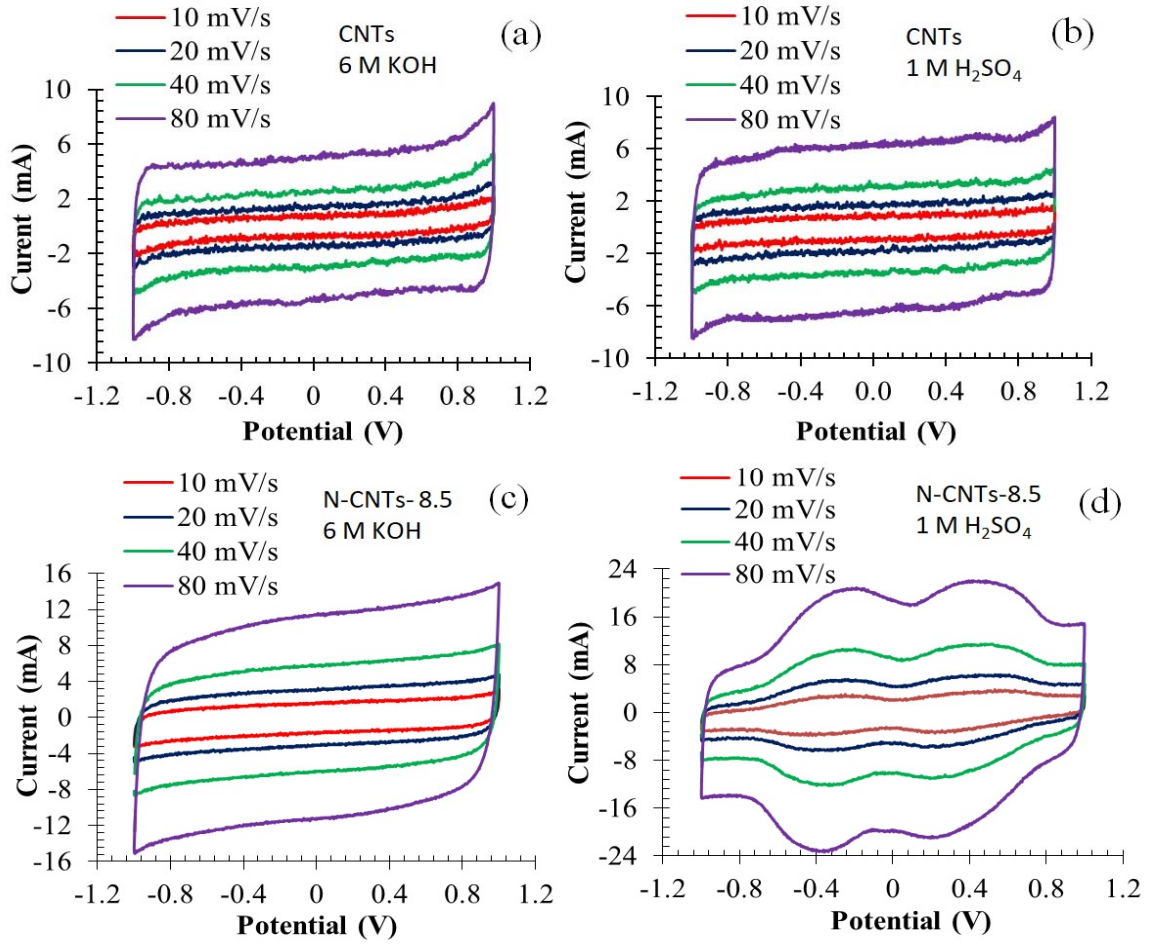

Fig. 6. CVs curves of SC cells with the electrodes made of undoped initial nanotubes (a, b) and nitrogen-doped nanotubes exemplified by N-CNTs-8.5 (c, d) in alkaline (a, c) and acid (b, d) electrolytes at the indicated potential scanning rates of 10, 20, 40 and 80 mV/s.

In both the alkaline (Fig. 6a) and acid electrolytes (Fig. 6b), distinct pseudocapacitance peaks are not observed on the CVs curves of SC cells with the electrode materials based on CNTs. The shape of the curves is close to rectangular; hence, the main contribution to capacitance is caused by the formation of electrical double layer and charge accumulation at the electrode/electrolyte interface.

Figures 6c and d show typical voltammetric curves for an electrode material that is based on nitrogen-doped nanotubes exemplified by N-CNTs-8.5 in different electrolytes. Other samples have similar shapes of the curves that differ in intensity of the peaks and in the area limited by the curves.

It is seen that functionalization of nanotubes with nitrogen increases the area limited by CVs curves, and hence the total capacitance of related electrode materials. Capacitance increases with the nitrogen content. Moreover, in the acid electrolyte (1 M aqueous solution of H_2SO_4) distinct pseudocapacitance peaks show up on CVs curves (Fig. 6d), whereas in the alkaline electrolyte (6 M aqueous solution of KOH) such peaks are not observed (Fig. 6c). Thus, nitrogen-doped nanotubes accumulate charge due to both the electrical double layer at the electrode/electrolyte interface and the redox processes with participation of nitrogen-containing groups (pseudocapacitance). Capacitance in the acid electrolyte is higher than in the alkaline one, which also agrees with the literature data.

The total capacitance in acid and alkaline electrolytes and EDL capacitance in the acid electrolyte were calculated from voltammetric curves for all the tested systems at different potential scanning rates by the technique mentioned above.

Figures 7a and b display the capacitance of electrode materials based on initial carbon nanotubes versus the potential scanning rate in acid and alkaline electrolytes.

Experimental data for N-CNT samples were processed with subtraction of pseudocapacitance. Results of the calculation are illustrated on Fig. 8.

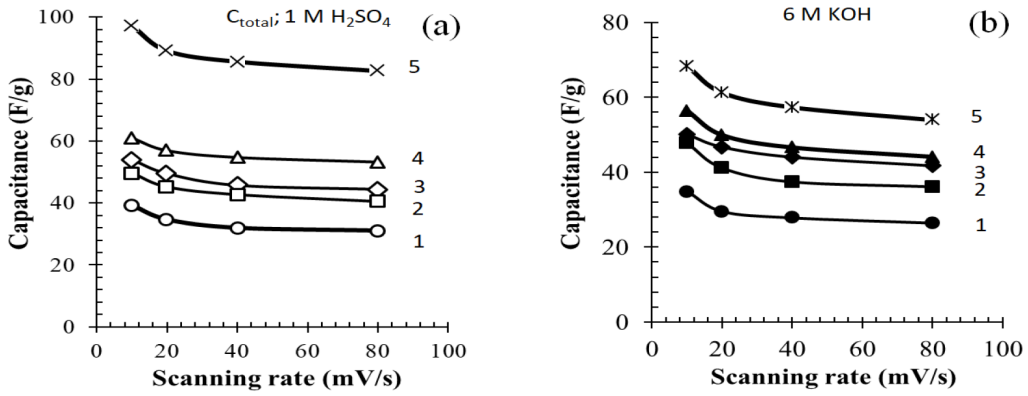

Fig. 7. Capacitance of electrode materials versus the scanning rate in a potential window from – 1 to + 1 V in acid (a) and alkaline (b) electrolytes. The electrode material: 1 – CNTs; 2 – N-CNTs-2; 3 – N-CNTs-3.6; 4 – N-CNTs-6; 5 – N-CNTs-8.5.

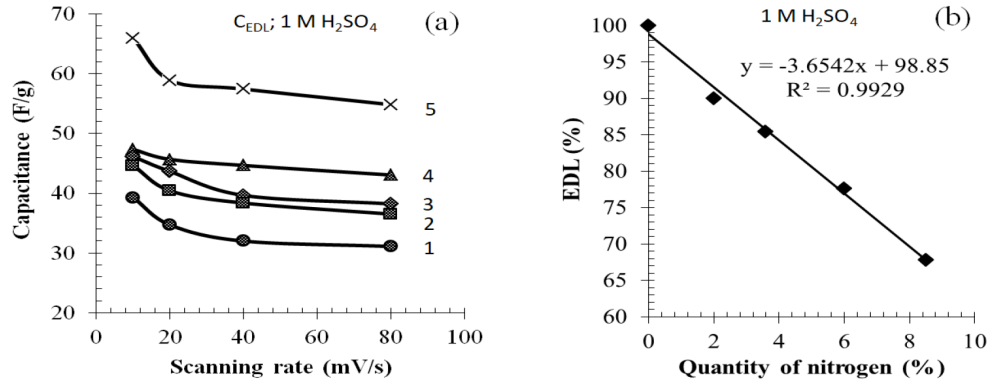

Fig. 8. Capacitance of electrical double layer after subtraction of pseudocapacitance (a) at different potential scanning rates; the contribution of EDL (%) in dependence on the nitrogen content in nitrogen-doped nanotubes at 10 mV/s (b). The electrode material: 1 – CNTs; 2 – N-CNTs-2; 3 – N-CNTs-3.6; 4 – N-CNTs-6; 5 – N-CNTs-8.5.

The dependences of EDL capacitance in the acid electrolyte on the potential scanning rate are displayed on Fig. 8a. The highest capacitance of 97 F/g (including the EDL capacitance of 65 F/g) is observed for N-CNTs-8.5 as an electrode material in 1 M H_2SO_4 solution, while the lowest capacitance (39 F/g in 1 M H_2SO_4 and 35 F/g in 6 M KOH) is observed for initial undoped CNTs. Hence, nitrogen doping of carbon nanotubes increases the capacitance by a factor of 1.3–2.5. For all the tested systems, the capacitance of electrical double layer CEDL is higher as compared to the electrodes based on the initial nanotubes, and manifestation of pseudocapacitance further increases the total capacitance C_{total}. However, an increase in the nitrogen content decreases the EDL contribution (%) to the total capacitance and increases the contribution of pseudocapacitance (Fig. 8b) to ~ 32% at the nitrogen content of 8.5 wt.% in the acid electrolyte.

3.2. Investigation of charge-discharge characteristics of electrode materials at a constant current

Charge-discharge curves of SC cells with the electrode materials based on undoped and nitrogen-doped nanotubes (samples with 3.6 and 8.5% nitrogen content) in acid and alkaline electrolytes are displayed on Fig. 9a and c.

Equivalent series resistance of SC cells and electric capacitance were calculated from GSCD curves (Figs. 9b and d). As the nitrogen content increases, the internal resistance of a cell decreases, whereas the capacitance increases. In the acid electrolyte the capacitance is higher, while the resistance is lower as compared to the alkaline electrolyte. Thus, studies in the acid electrolyte are more promising. The results obtained agree with CVs data.

One can see that in the acid electrolyte (1 M H_2SO_4 solution, Fig. 10a and b) the impedance values are lower than in the alkaline electrolyte for all the studied systems. Nitrogen doping of nanotubes facilitates a decrease in the full impedance of SC cells, mostly in its reactive (capacitance) component; this testifies to a higher capacitance of nitrogen-doped nanotubes as an electrode material, which is consistent with CVs and GSCD data. However, in the alkaline electrolyte, nitrogen-doped samples show an increase in the active component of impedance (Fig. 10c); this component increases with the nitrogen content in nanotubes, which may be related to electrical conductivity of the materials.

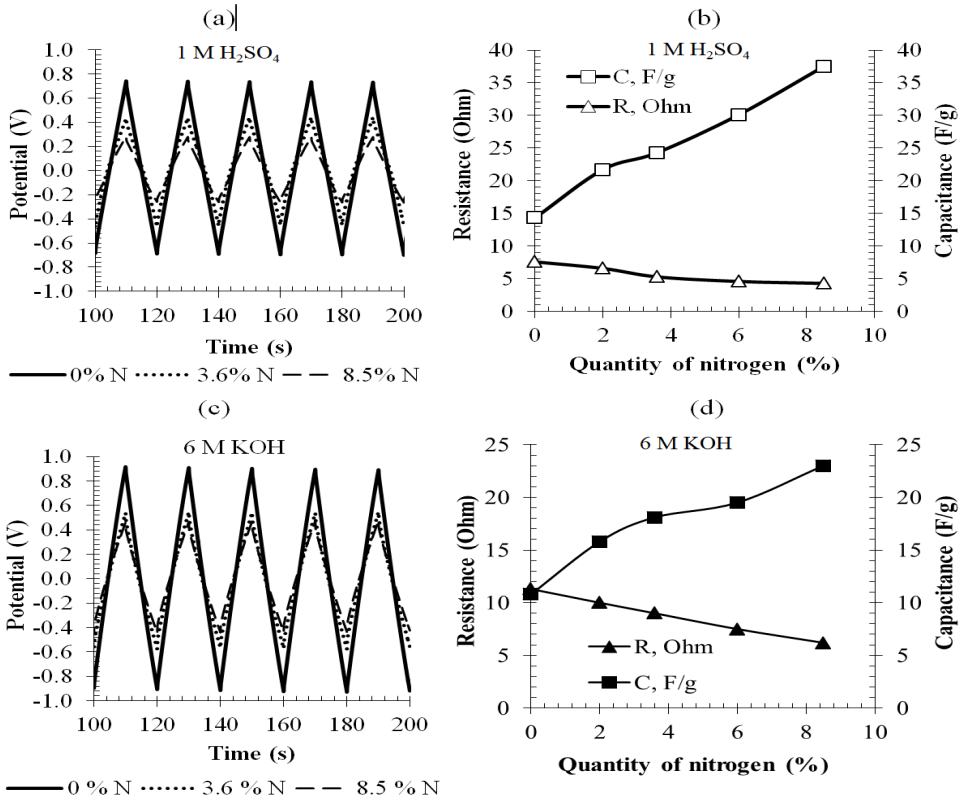

Fig. 9. GSCD curves for SC cells with the electrode materials based on undoped and nitrogen-doped nanotubes in acid (a) and alkaline (c) electrolytes, and dependences of electrode capacitance and equivalent series resistance, which were calculated from GSCD curves, in acid (b) and alkaline (d) electrolytes.

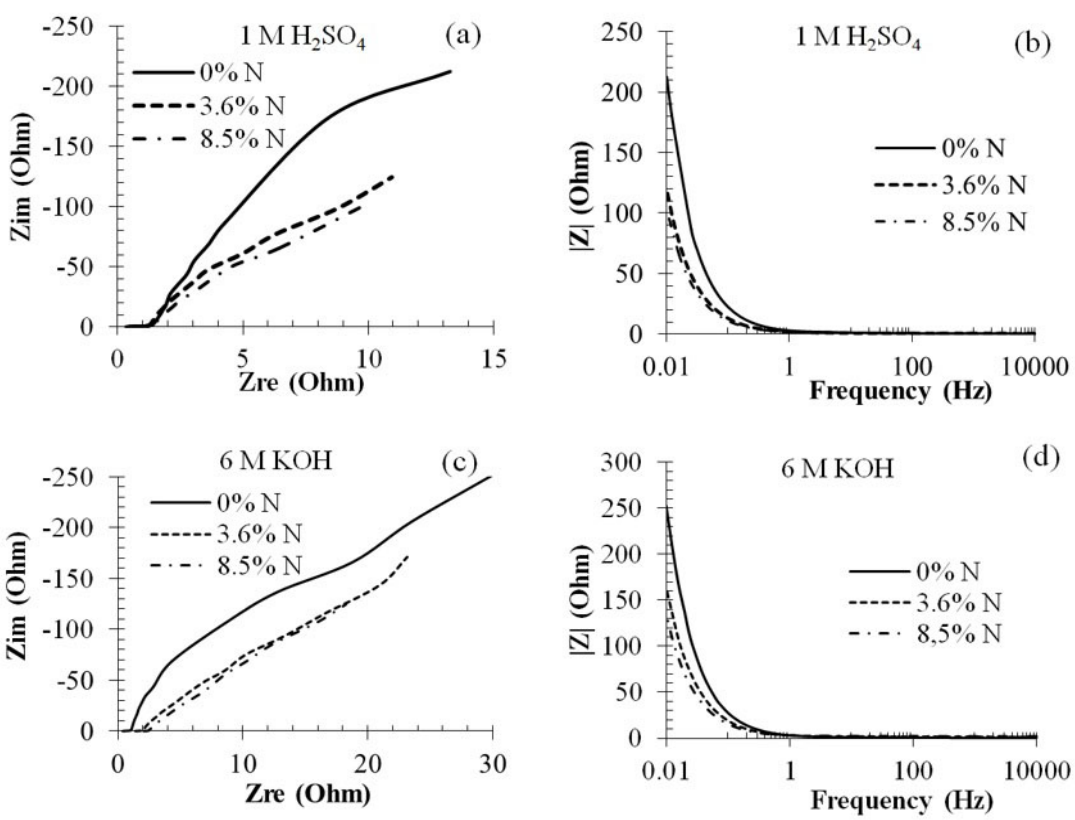

Fig. 10. The Nyquist diagrams (a, c) and dependences of the full impedance of a cell on the frequency (b, d) of symmetric cells with the electrodes based on undoped and nitrogen-doped nanotubes in acid (a, b) and alkaline (c, d) electrolytes. Nitrogen content in N-CNTs is indicated on the plots.

4. Conclusions

A comprehensive technique for electrochemical studies of electrode materials has been developed. It includes estimation of the contribution of EDL capacitance and pseudocapacitance to the total capacitance from the area of CVs curves and a comparison of the obtained data with chronopotentiometry and impedometry data. The measurements were made in a specially devised two-electrode electrochemical cell using different electrolytes: acid – 1 M aqueous H_2SO_4 solution, and alkaline – 6 M aqueous KOH solution on a PARSTAT 4000 potentiostat/galvanostat. Electrode materials were represented by undoped (CNTs) and nitrogen-doped (N-CNTs) nanotubes containing 2, 3.6, 6 or 8.5% nitrogen. A technique for processing of CVs curves was developed to take into account the contribution from capacitance of electrical double layer and pseudocapacitance to the total capacitance of the tested systems by subtraction of pseudocapacitance.

The analysis of CVs curves obtained in the acid electrolyte demonstrated that nitrogen doping of nanotubes increases the capacitance of electrical double layer at the electrode/electrolyte interface and pseudocapacitance as a result of electrochemical processes involving nitrogen-containing groups, thus increasing the total capacitance by a factor of 1.3–2.5. Pseudocapacitance peaks are not observed for undoped nanotubes in the acid electrolyte. As the nitrogen content is increased, the percent contribution of EDL to the total capacitance decreases, and the dependence is rectilinear; however, the calculated EDL capacitance increases in the process. Thus, pseudocapacitance is caused by the nitrogen-containing groups. In the alkaline electrolyte, pseudocapacitance peaks are not observed for all the tested systems; so the capacitance is caused mostly by the formation of electrical double layer. However, in this case, the highest capacitance is observed also for nitrogen-doped nanotubes and increases with their nitrogen content. The optimal nitrogen content was 8.5%. Such systems typically retain the shape of the curves and positions of pseudocapacitance peaks when the potential scanning rate is varied from 10 to 80 mV/s. Therewith, the percent contribution of pseudocapacitance virtually does not change, which indicates the occurrence of fast and kinetically uninhibited redox processes involving nitrogen-containing groups; this is confirmed by

the absence of peaks in the high-frequency (kinetic) region of the Nyquist diagrams that are typical of the majority of pseudocapacitance materials.

Thus, the application of the developed technique for measuring the capacitance characteristics made it possible: 1) to reveal the possibility of finding two capacitance components: the EDL capacitance and pseudocapacitance; 2) to quantitatively determine the contribution from EDL capacitance.

As a result, it was found that nitrogen-doped nanotubes (especially N-CNTs-8.5) open up ample opportunities for their use as a material of the working electrode in supercapacitors owing to a relatively high capacitance (including the EDL capacitance, pseudocapacitance and total capacitance) and stability in cycling.

Acknowledgements

This publication has emanated from research conducted with financial support of the Russian Science Foundation (Grant No. 15-13-10043).

References

[1]. M.S. Ribeiro, A.L. Pascoini, W.G. Knupp, I. Camps, *Appl. Surf. Sci.* 426 (2017) 781–787. DOI:10.1016/j.apsusc.2017.07.162

[2]. L. Sun, X. Wang, Y. Wang, Q. Zhang, *Carbon* 122 (2017) 462–474. DOI: 10.1016/j.carbon.2017.07.006

[3]. S. Merum, J.B. Veluru, R. Seeram, *Mater. Sci. Eng. B* 223 (2017) 43–63. DOI: 10.1016/j.mseb.2017.06.002

[4]. W. Zhai, N. Srikanth, L.B. Kong, K. Zhou, *Carbon* 119 (2017) 150–171. DOI: 10.1016/j.carbon.2017.04.027

[5]. D. Zhong, Z. Zhang, L.-M. Peng, *Nanotechnology* 28 (2017) Article number: 212001. DOI: 10.1088/1361-6528/aa6a9e

[6]. Gaurav Bhanjana, Neeraj Dilbaghi, Ki-Hyun Kim, Sandeep Kumar, *J. Mol. Liq.* 242 (2017) 966–970. DOI: 10.1016/j.molliq.2017.07.072

[7]. V.V. Chesnokov, O.Yu. Podyacheva, Z.R. Ismagilov, *Chemistry for Sustainable Development* 24 (2016) 521–527. DOI: 10.15372/KhUR20160412

[8]. V.V. Chesnokov, O.Yu. Podyacheva, A.N. Shmakov, L.S. Kibis, A.I. Boronin, Z.R. Ismagilov, *Chinese J. Catal.* 37 (2016) 169–176. DOI: 10.1016/S1872-2067(15)60982-2

[9]. A.N. Suboch, S.V. Cherepanova, L.S. Kibis, D.A. Svintsitskiy, O.A. Stonkus, A.I. Boronin, V.V. Chesnokov, A.I. Romanenko, Z.R. Ismagilov, O.Yu. Podyacheva, *Fullerenes, Nanotubes Carbon Nanostruct.* 24 (2016) 520–530. DOI: 10.1080/1536383X.2016.1198331

[10]. Z.R. Ismagilov, A.E. Shalagina, O.Yu. Podyacheva, R.I. Kvon, I.Z. Ismagilov, M.A. Kerzhentsev, Ch.N. Barnakov, A.P. Kozlov, *Kinet. Katal.* 48 (2007) 581–588. DOI: 10.1134/S0023158407040179

[11]. N.K. Eremenko, O.Yu. Podyacheva, Z.R. Ismagilov, I.I. Obraztsova, A.N. Eremenko, L.S. Kibis, D.A. Svintsitskiy, *Eurasian Chem.-Technol. J.* 17 (2015) 101–103. DOI: 10.18321/ectj200

[12]. Y.G. Kryazhev, V.A. Drozdov, V.S. Solodovnichenko, I.V. Anikeeva, V.A. Likholobov, Z.R. Ismagilov, O.Y. Podyacheva, R.I. Kvon, *Solid Fuel Chem.* 49 (2015) 1–6. DOI: 10.3103/S0361521915010073

[13]. O.Yu. Podyacheva, Z.R. Ismagilov, *Catal. Today* 249 (2015) 12–22. DOI: 10.1016/j.cattod.2014.10.033

[14]. O.Yu. Podyacheva, S.V. Cherepanova, A.I. Romanenko, L.S. Kibis, D.A. Svintsitskiy, A.I. Boronin, O.A. Stonkus, A.N. Suboch, A.V. Puzynin, Z.R. Ismagilov, *Carbon* 122 (2017) 475-483. DOI: 10.1016/j.carbon.2017.06.094

[15]. O.Yu. Podyacheva, Z.R. Ismagilov, R.A. Buyanov, *Chemistry for Sustainable Development* 24 (2016) 57–60. DOI: 10.15372/KhUR20160108

[16]. A.N. Suboch, L.S. Kibis, O.A. Stonkus, D.A. Svinitskiy, A.B. Ayushev, Z.R. Ismagilov, O.Yu. Podyacheva, *Chemistry for Sustainable Development* 25 (2017) 85–91. DOI: 10.15372/KhUR20170112

[17]. Shuai Ban, Jiujun Zhang, Lei Zhang, Ken Tsay, Xinfu Zou, *Electrochim. Acta* 90 (2013) 542–549. DOI: 10.1016/j.electacta.2012.12.056

[18]. A.V. Puzynin, B.P. Aduev, G.M. Belokurov, A.P. Kozlov, O.S. Efimova, A.V. Samarov, Ch.N. Barnakov, Z.R. Ismagilov, *Vestnik KuzGTU* [KuzSTU Bulletin] 5 (99) (2013) 62–67 (in Russian).

[19]. A. González, E. Goikolea, J.A. Barrena, R. Mysyk, *Renew. Sust. Energ. Rev.* 58 (2016) 1189–1206. DOI: 10.1016/j.rser.2015.12.249

[20]. H.J. Zheng, A.M. Yu, C.A. Ma, *Russ. J. Electrochem.* 48 (2012) 1179–1186. DOI: 10.1134/S102319351205014X

[21]. V.M. Zhukovskiy, O.V. Bushkova. Impedance spectroscopy of solid electrolytic materials; Ural State University, Ekaterinburg, Russia, 2000, 35 p. (in Russian).

[22]. E. Barsoukov, J.R. Macdonald. Impedance Spectroscopy: Theory, Experiment, and Applications; Wiley-Interscience, N.Y., 2005, 606 p.

[23]. A.S. Kavasoglu, N. Kavasoglu, S. Oktik, *Solid-State Electron.* 52 (2008) 990–996. DOI: 10.1016/j.sse.2008.02.004